Uptake and Collision Dynamics of Gas Phase Ozone at Unsaturated Organic Interfaces

John Vieceli, Odette L. Ma, and Douglas J. Tobias*

Department of Chemistry, University of California, Irvine, California 92697-2025

Received: February 5, 2004; In Final Form: April 26, 2004

The uptake of gas phase ozone and the collision rate between ozone and double bonds at three different unsaturated organic interfaces with vapor are studied using classical molecular dynamics computer simulations. The organic systems are a self-assembled monolayer of 1-octenethiolate molecules adsorbed on a gold surface, liquid 1-tetradecene, and a monolayer of 1-oleoyl-2-palmitoyl-*sn*-glycero-3-phosphocholine molecules adsorbed at the water liquid/vapor interface. The structural features of the neat organic systems are characterized and correlated with the dynamics in the presence of gas phase ozone molecules. The collision rate between ozone and a double bond is sensitive to several factors, including the extent of localization of the double bonds in the system and the distance that ozone diffuses into the organic phase. However, the average lifetime of a collision between ozone and a double bond is independent of the organic system. A comparison of the simulation results with experimental results from these systems shows good agreement. The results are discussed in the context of the oxidative processing of organic aerosols in the atmosphere.

I. Introduction

In recent years, there has been increasing interest in characterizing the reactivity of gases at aqueous and organic interfaces with air. One fundamental reason for this is a growing amount of evidence from experiments, molecular simulations, and kinetic modeling that indicates that the interface between two phases is a unique region where the kinetics and mechanisms of chemical processes differ from those in bulk solutions or the gas phase.[1−4] However, the difference between a heterogeneous reaction and the same reaction occurring in a bulk liquid or the gas phase may arise for different reasons. One is that a reactive species in solution exhibits a surface excess, in which case it is preferentially located at the interface for reaction with an incoming gas phase reactant. Another reason is that the incoming gas phase species is trapped at the interface during the uptake process. Also, the activation energy barrier for the reaction at the interface may be altered. Finally, one of the reactive species may be oriented in a heterogeneous environment in such a way that the reaction occurs more readily than in the gas or bulk liquid phases. Predicting the most relevant factors that alter the outcome of a particular heterogeneous reaction from the outcome of the same chemical reaction occurring in a bulk liquid or the gas phase is an open problem.

One class of heterogeneous chemical processes, which is particularly important to environmental and biological systems, is the reaction of atmospheric oxidants with unsaturated organic surfaces. This is due to the abundance of interfaces between an organic phase and air in nature. For example, in atmospheric chemistry, organic matter has been identified as a significant contribution to tropospheric aerosols.[5−7] Chemical reactions of organic aerosols with atmospheric oxidants potentially affect the climate by altering the properties of the aerosols, such as a propensity to uptake water and nucleate cloud formation.[8] Also, the reactions result in the release of volatile products to the gas phase. Organic compounds are also present in the environment in a surface layer on bodies of water, which is generated from the decomposition of biological matter.[9] The organic surface layer is also subject to oxidation by gas phase species, thus altering the compounds dissolved in the water and the compounds released into the atmosphere.

Organic films in living organisms are exposed to oxidants in the atmosphere. For example, a surfactant mixture of phospholipids and proteins is present at the air/liquid interface of the lungs.[10] The surfactant is responsible for reducing the surface tension to near zero, which facilitates the expansion and contraction of the lungs during inhalation and exhalation. Certain respiratory diseases are correlated with the degradation of the pulmonary surfactant, where a possible mechanism for the degradation is oxidation by pollutants in inhaled air.[11] Unsaturated phospholipids that are present in plants and trees are subject also to oxidative processing by atmospheric gases.[12] A potential site for damage is the phospholipid bilayer that composes the cell membranes of guard cells located in the lower epidermis of leaves.[13] Guard cells are responsible for opening and closing the pores that allow gas exchange with the atmosphere.

There are several pollutants present in the atmosphere that can contribute to the oxidative processing of the organic surfaces discussed above, such as ozone, hydroxyl, nitrate radicals, and atomic halogens. The reactive uptake of ozone at unsaturated organic surfaces has been studied extensively in experiments.[2,4,14−23] For a complete review of experiments involving organic aerosol chemistry, a recent article written by Rudich is available.[24] Various models for the organic component are used in these experiments, including liquid/vapor interfaces, self-assembled monolayers, aerosol particles, and organic thin films adsorbed at the liquid/vapor interface of water. In general, the model selection is made so that the essential features of a naturally occurring system are captured. From these experiments, the uptake probability of ozone and the products from the reaction of ozone with a double bond have been characterized for a variety of unsaturated organic surfaces. Ozone reacting with alkenes has received a considerable amount of attention for several reasons. Ozone is present in the troposphere in a

* To whom correspondence should be addressed. E-mail: dtobias@uci.edu.

10.1021/jp0494584 CCC: $27.50
Published on Web 06/04/2004

concentration range of 30−40 ppb,[25] and alkenes are a common functional group present in the environmental and biological systems mentioned above. Also, the reaction mechanism of ozone with alkenes in bulk liquids and in the gas phase is well characterized,[25] which provides a basis for understanding the effects of a heterogeneous environment on the reaction. Finally, ab initio calculations of ozone reacting with various alkenes have been performed.[26,27] Although valuable information regarding ozone uptake and reactivity at organic surfaces containing alkenes has been obtained from experiment and theory, very little dynamic information at a molecular level is available.

Molecular dynamics (MD) computer simulations are a methodology by which chemical structure and dynamics can be studied from a molecular perspective and correlated with experimental results. MD simulations have been used previously to study the kinetics and mechanisms of atomic and molecular uptake and reactivity at aqueous,[28,29] aqueous halide,[30] and organic surfaces.[31−35] One focus of some of these simulations is to quantify the probability of a gas phase species with a thermal impact velocity being absorbed into a bulk solution by simulating the process directly[28,30,34] or by calculating the free energy profile for the process.[28,29] Another focus of these studies is on the relationship between surface structure and energy transfer, and excellent agreement with experimental measurements of the trapping probability, fractional energy loss, and angular distribution of the scattered species was found.[31−33,35] All of these studies demonstrate the utility of classical MD simulations in gaining a molecular perspective of the uptake of gases at various types of liquid surfaces.

In the present paper, MD simulations are used to study the uptake of gas phase ozone and the ozone−double bond collision dynamics at organic surfaces containing alkenes. Three different organic substrates at the interface with vapor are simulated with and without gas phase ozone present. The organic substrates include a self-assembled monolayer (SAM) composed of 1-octenethiolate, the liquid/vapor interface of 1-tetradecene (C14ENE), and a phospholipid monolayer of 1-oleoyl-2-palmitoyl-*sn*-glycero-3-phosphocholine (OPPC) molecules adsorbed at the water liquid/vapor interface. The main purpose of these simulations is to correlate the organic structure with the ozone uptake and collision dynamics. For example, how does the organic density at the surface affect the uptake of ozone into the interior of the organic phase? Also, how does double bond exposure at the surface and the localization of double bonds in the system affect the collision dynamics with ozone? The selection of these three organic systems interacting with gas phase ozone is guided by the fact that experiments on each system have been performed.[2,15,16,19] Another purpose of the simulations is to complement the results and conclusions of these experiments with a molecular level perspective. The simulation results presented in this work also contribute to a general understanding of the relevant structural and dynamic factors in heterogeneous chemical processes.

The results from the simulations of the neat systems show that the structure of the OPPC monolayer is similar to the C14ENE liquid system, whereas the SAM structure is more similar to a solid surface. In the presence of ozone, the organic density at the interface determines whether uptake into the organic phase occurs, and as a result, this determines the residence time of the ozone molecules. Because uptake into the organic phase does not occur in the SAM system because of the large alkene carbon density at the surface, a residence time that is a factor of 3 smaller than the residence times in the C14ENE and OPPC systems is observed. The collision rate between ozone and double bonds is the largest in the C14ENE liquid system because of uptake into the bulk liquid and double bonds dispersed throughout the organic phase. Localization of the double bonds in a region of the SAM and OPPC monolayer systems results in a smaller collision rate than in the liquid system. Although the collision rate is sensitive to the structure of the organic system, the collision lifetime is independent of the organic system being considered.

In section II, the simulation models for the three organic systems and ozone are described. The simulation methodology is given in section II also. The results are discussed in section III, followed by conclusions and atmospheric implications in section IV.

II. Systems and Methods

A. Neat Systems. *1. Self-Assembled Monolayer.* The SAM consists of 64 1-octenethiolate ($S(CH_2)_6CH{=}CH_2$) molecules adsorbed on a gold (111) surface in a simulation box geometry of 40.08 Å (x) × 34.72 Å (y) × 62.00 Å (z). The z dimension is normal to the SAM/vapor interface. This geometry yields a surface area of 22 Å^2/molecule and approximately 40 Å of vapor adjacent to the SAM surface in the z dimension. The system is constructed from a self-assembled monolayer composed of octadecanethiolate molecules by removing the last 10 carbons and modifying carbon types one and two from sp^3 to sp^2. The hydrocarbon force field is taken from a publication by Tobias, Tu, and Klein,[36] and the adsorption potential and surface corrugation potential are taken from the work of Mar and Klein.[37] A 400 ps equilibration and an 800 ps simulation of the neat system are run using CHARMM.[38]

2. 1-Tetradecene Liquid/Vapor Interface. The neat liquid slab of 1-tetradecene ($CH_3(CH_2)_{11}CH{=}CH_2$) consists of 384 $C_{14}H_{28}$ molecules in a simulation box of dimensions 54.52 Å (x) × 54.52 Å (y) × 150 Å (z). There are two liquid/vapor interfaces present in the xy plane on each side of a 50 Å thick bulk liquid lamella. The initial configuration of the system is derived from a box of liquid tetradecane by modifying carbons types one and two from sp^3 to sp^2. The CHARMM27 force field is used to model the hydrocarbon molecules.[39] PINY_MD is used to generate a 400 ps equilibration of this system, followed by a 400 ps simulation.[40] The simulation length is half that used in the SAM system because there are two liquid/vapor interfaces from which the equilibrium averages are obtained. Properties of the bulk liquid and interface calculated using this model are in reasonable agreement with experimental values. These include the bulk liquid density (simulation at 300 K: 0.72 g/mL; experimental at 293 K: 0.77 g/mL)[41] and the surface tension (simulation at 300 K: 21 mN/m; experimental at 303 K: 26 mN/m).[42]

3. Phospholipid Monolayer. Simulation details of neat OPPC systems are available in a previous publication by Wadia et al. that was focused on the structure of two different monolayer compressions in relation to experiments of ozone reactivity with OPPC monolayers.[2] A monolayer compression of 80 Å^2/lipid is selected to study the uptake and collision dynamics of gas phase ozone with alkenes. Briefly, a lipid monolayer is placed on each side of a 20 Å thick slab of 2258 water molecules with the phosphocholine headgroups immersed in the water phase and the hydrocarbon tails projecting into the vapor phase. Each monolayer consists of 36 OPPC molecules. The simulation box geometry is 53.66 Å (x) × 53.66 Å (y) × 100 Å (z), where the z dimension is perpendicular to the OPPC/water interface.

B. Ozone. In the SAM system, four ozone molecules are uniformly distributed in the xy plane approximately 20 Å above

the SAM surface in the *z* dimension. A reflecting wall is placed at $z = 62$ Å to prevent the escape of gas phase ozone molecules. In the C14ENE and OPPC systems, eight ozone molecules are uniformly distributed in the gas phase of each system by placing four ozone molecules above each interface. The ozone molecules are added to the final configurations from the simulations of the neat systems.

The force field for the ozone molecules is built from the CHARMM22 force field.[43] Each oxygen atom of ozone is assigned parameters of a carbonyl oxygen atom with no atomic charges. This atomic charge selection is based on the small value of the experimental molecular dipole moment, which is 0.53 D,[44,45] and the nonpolar nature of the organic systems. The equilibrium internal geometry of the ozone molecule is taken from the gas phase, where the two bond lengths are 1.278 Å and the bond angle is 117°.[46]

Following a 300 ps equilibration in each system, a 1600 ps simulation of the SAM system with ozone is run using CHARMM,[38] and an 800 ps simulation is run in the C14ENE and OPPC systems with ozone using PINY_MD.[40] The simulation time is doubled in the SAM system because there is one interface with four ozone molecules relative to two interfaces with eight ozone molecules in the other two systems.

The model used in these simulations does not incorporate the reaction between ozone and double bonds to form the primary ozonide.[25] The inclusion of reactive chemistry in computer simulations with a large number of atoms is a complicated problem,[47] and a simpler approach to gaining information about the reaction rate is used here. The reaction rate, *R*, is related to the collision rate, *C*, by the expression

$$R = C \times \Gamma \tag{1}$$

where Γ is the reaction probability. The collision rate is determined from the equilibrium simulations in the presence of ozone, given that a reliable definition of the distance between ozone and a double bond for a collision event can be obtained. Multiple ozone molecules are included in each system to reduce the amount of time required to obtain a converged collision rate. With the collision rate from simulation, the applicability of gas−surface collision theory to these systems can be tested. Also, if the experimental reaction rate is known, then the collision rate from simulations can be used, according to eq 1, to estimate the reaction probability.

C. Simulation Details. All of the simulations described above are performed with a constant number of molecules, temperature, and volume. The temperature of 300 K is controlled in each system using Nose-Hoover chain thermostats.[48] The smooth particle mesh Ewald method is used to calculate the electrostatic interactions.[49] The real space part of the Ewald sum and the van der Waals interactions are truncated at 10 Å with a spherical truncation scheme. An integration time step of 1.0 fs is used in the SAM simulations, and a 4.0 fs time step with multiple time-step integration[48] is selected for the C14ENE and OPPC simulations to balance the large system sizes with reasonable computational times. All bond lengths involving hydrogen atoms are constrained to the equilibrium values using the SHAKE/RATTLE algorithm.[50,51]

III. Results and Discussion

A. Neat Systems. The results from simulations of the neat systems are used to characterize the structural features of the organic substrates that are relevant to the uptake of ozone and the ozone−double bond collision dynamics. One snapshot of each system from the neat simulation is shown in Figure 1,[52]

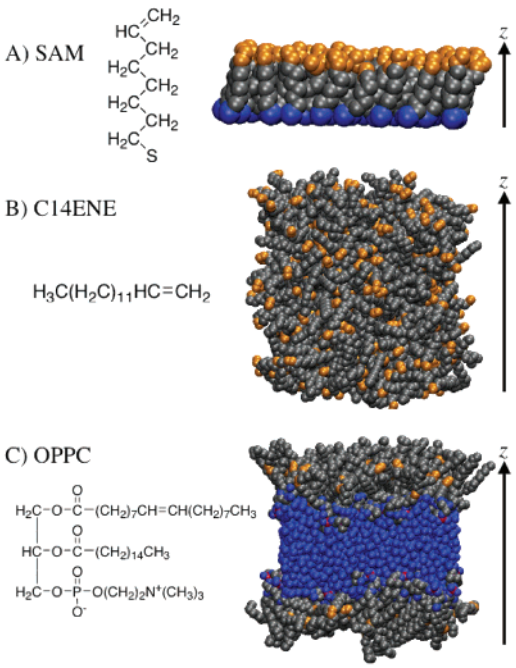

Figure 1. Molecular bonding structures and snapshots from the molecular dynamics trajectories for the (A) SAM, (B) C14ENE, and (C) OPPC systems. In each snapshot, the *z* dimension, which is in the plane of the page, is perpendicular to the interface with the vapor phase. The alkene carbons are orange, all other carbons are gray, and the hydrogen atoms are removed for clarity. (A) Sulfur (blue). (C) Phosphorus (red); oxygen (blue); nitrogen (purple). The snapshots are not scaled in size relative to one another.

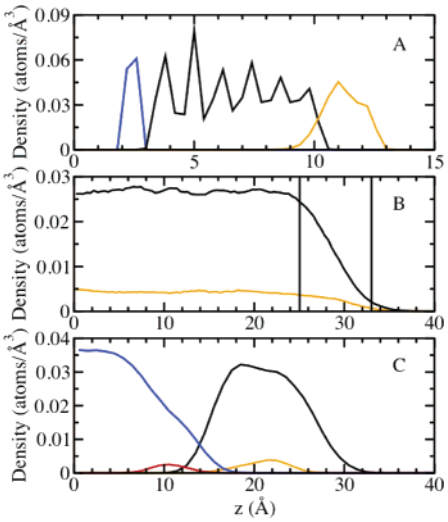

Figure 2. Atomic density profiles in the direction normal to the interface between the vapor phase and the organic media for the neat (A) SAM, (B) C14ENE, and (C) OPPC systems. In each panel, the alkene carbons are orange, and the alkane carbons are black. (A) Sulfur (blue). (B) Liquid/vapor interface of C14ENE defined by the vertical lines at $z = 25$ and 33 Å. (C) Phosphorus (red); oxygen from water (blue). Note the different scales in each panel.

where the *z* dimension is perpendicular to the interface with the vapor phase. To clarify the location of the double bond in each molecule, the chemical bonding structure is shown in Figure 1 also. The phosphocholine headgroups in the OPPC snapshot are difficult to view because they are embedded in the water phase. The atomic density profiles in the *z* dimension are shown in Figure 2 for the SAM (top panel), C14ENE (middle panel), and OPPC (bottom panel) systems.[2] In the SAM system, there is one SAM/vapor interface, and the location of

the gold surface corresponds to $z = 0$ Å. In the C14ENE and OPPC systems, there are two interfaces with the vapor, and the density profile is obtained by averaging over both interfaces, where the abscissa corresponds to the distance from the system center of mass position in the z dimension. This procedure of averaging over both interfaces is used to represent the data from the C14ENE and OPPC systems in the remainder of this paper. The vertical lines in the C14ENE density profile at $z = 25$ and 33 Å correspond to the z coordinate at 90 and 10%, respectively, of the C14ENE liquid density, which operationally defines the interface region.

The location and magnitude of the alkene carbon density are directly relevant to the ozone−double bond collision dynamics. Although the alkene carbons are dispersed throughout the C14ENE system, as is expected for a liquid, the alkene carbons are located in a narrow region of the z dimension in the SAM and OPPC systems.[2] This is due to an interaction with a substrate that restricts the molecular orientations sampled in these two systems. (See below.) The terminal double bond of 1-octenethiolate places the alkene carbons adjacent to the vapor phase in the SAM system, and the internal double bond of the OPPC molecule separates the alkene carbons from the vapor phase by approximately 5−10 Å of alkane carbon. Collisions between ozone and double bonds can occur directly at the SAM surface, but these collisions must be preceded by the uptake of ozone into the interior of the OPPC monolayer. One reason for the order of magnitude difference between the peaks of the alkene carbon density profiles in the SAM and OPPC systems is a smaller surface area per double bond in the SAM system (22 Å^2/double bond) relative to that in the OPPC system (80 Å^2/double bond). The C14ENE system is unique because the potential for ozone−double bond collisions exists both at the liquid surface and in the bulk.

The total carbon density in the bulk of the C14ENE system (0.031 atoms/Å^3) is similar to the total carbon density in the interior of the OPPC monolayer (0.033 atoms/Å^3). Although the OPPC system contains a monolayer of hydrocarbon tails, these hydrocarbons pack to yield a density profile that is more similar in shape and magnitude to a liquid hydrocarbon than a SAM. This suggests that the range of orientations sampled by the lipid portion of the OPPC molecules is larger than that sampled by the 1-octenethiolate molecules of the SAM. This is confirmed by calculating the probability distribution of the angle between a selected molecular vector and the interface normal in each system, $P(\theta)$. These distributions are shown in Figure 3 for the three different systems. The molecular vectors are defined in the figure caption. The probability distribution in the SAM system (top panel) peaks near $\theta = 15°$ and is populated up to approximately $\theta = 35°$. This is in reasonable agreement with the 26−28° angle between the surface normal and alkyl chains in self-assembled monolayers of thiolates on gold measured by FTIR.[53] However, it is narrower than the distribution shown in Figure 3 for the lipid portion of the OPPC system (bottom panel), which is populated from $\theta = 0$ to 75°. The smaller surface area per molecule in the SAM system results in a densely packed monolayer with solidlike characteristics compared to the OPPC monolayer, which has a larger surface area per molecule and more liquidlike characteristics.

In the C14ENE system, the three probability distributions in the middle panel of Figure 3 correspond to three 5 Å thick layers of the liquid slab near the liquid/vapor interface, as explained in the figure caption. The distribution for the layer nearest the bulk is flat and represents the distributions obtained from the bulk liquid. As the vapor is approached from the bulk liquid,

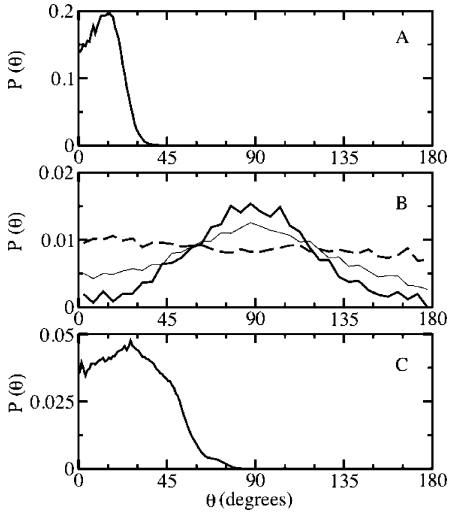

Figure 3. Probability distributions of the angle between a selected molecular vector and the interface normal in the neat (A) SAM, (B) C14ENE, and (C) OPPC systems. 0° corresponds to the molecular vector parallel to the interface normal. (A) Molecular vector drawn from the sulfur atom to the terminal carbon atom. 0° corresponds to the sulfur atom being closer to the gold surface. (B) Distributions for molecules with a center of mass z coordinate that are 20−25 Å (dashed), 25−30 Å (thin solid), and 30−35 Å (thick solid) away from the z coordinate of the system center of mass. The molecular vector is drawn from C14 to C1. 0° corresponds to the C14 atom being closer to the z coordinate of the system center of mass. (C) Molecular vector drawn from the phosphorus atom to the terminal carbon atom of the palmitoyl chain. 0° corresponds to the phosphorus atom being closer to the z coordinate of the system center of mass. All of the distributions are normalized such that $\int_0^{180} P(\theta) \sin(\theta)\, d\theta = 1$. Note the different scales in each panel.

the most probable molecular orientation becomes perpendicular to the interface normal rather than random. This arrangement increases the van der Waals interaction between the organic molecules relative to that for the parallel orientation. The perpendicular orientation, which places the double bond in the plane of the interface, may result in a larger exposure of the double bonds to the gas phase than is expected from a random molecular orientation. (See below.)

The molecular orientation distribution yields information about the organic structure on a length scale of tens of angstroms. Structural data on a length scale of several angstroms that is relevant to the reactivity of ozone with double bonds is obtained from the double bond orientation distribution. A preferential double bond orientation may affect the reaction rate by modifying the number of collisions that are in the proper orientation for a reaction to occur. The probability distributions of the angle between the double bond vector and the interface normal, $P(\psi)$, are shown in Figure 4 for each system. The double bond vectors are defined in the figure caption. The distributions for the SAM and OPPC systems resemble the distributions obtained from the molecular vector shown in panels A and C of Figure 3 but are broader. In the C14ENE system, the three distributions shown correspond to the same three molecular layers in panel B of Figure 3. The double bonds at the liquid/vapor interface of the C14ENE system are oriented randomly, despite the fact that the molecules are lying flat on the surface.

Structural information about each system that is independent of the gas phase species being considered is obtained from the data in Figures 2−4. However, the structural environment that an incoming gas phase species encounters is dependent on the size of the species and the roughness of the surface. Snapshots

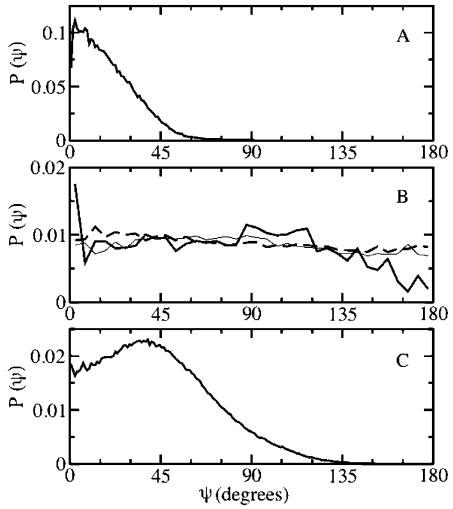

Figure 4. Probability distributions of the angle between the double bond vector and the interface normal in the neat (A) SAM, (B) C14ENE, and (C) OPPC systems. 0° corresponds to the bond vector parallel to the interface normal. (A) Molecular vector drawn from C2 to C1, where 0° corresponds to C2 being closer to the gold surface. (B) Distributions for molecules with a center of mass z coordinate 20−25 Å (dashed), 25−30 Å (thin solid), and 30−35 Å (thick solid) away from the z coordinate of the system center of mass. The molecular vector is drawn from C2 to C1, where 0° corresponds to C2 being closer to the z coordinate of the system center of mass. (C) Molecular vector drawn from C9 to C10 of the oleoyl chain, where 0° corresponds to C9 being closer to the z coordinate of the system center of mass. All of the distributions are normalized such that $\int_0^{180} P(\theta)\ \sin(\theta)\ d\theta = 1$. Note the different scales in each panel.

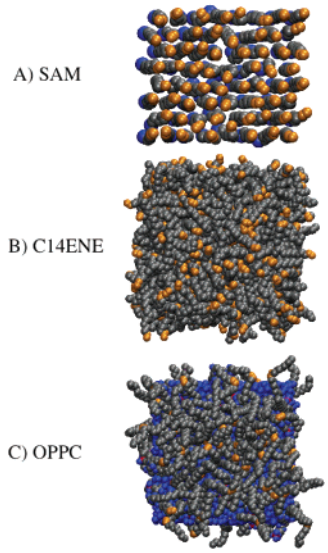

Figure 5. Different view of the same snapshots shown in Figure 1 for the neat (A) SAM, (B) C14ENE, and (C) OPPC systems. The perspective is from the vapor side of the interface in the direction of the z dimension. The colors correspond to the same atoms as in Figure 1, and the hydrogen atoms are removed for clarity. The snapshots are not scaled in size relative to one another.

of the neat systems from the vapor side of the interface in the direction of the z dimension are shown in Figure 5.[52] These snapshots yield a qualitative picture of the environment that an ozone molecule encounters upon striking the organic surface. A single quantity that represents the average exposure of a reactive site to an approaching gas phase species of a given size can be obtained using the solvent accessible surface area (SASA) analysis developed by Lee and Richards.[54] For the

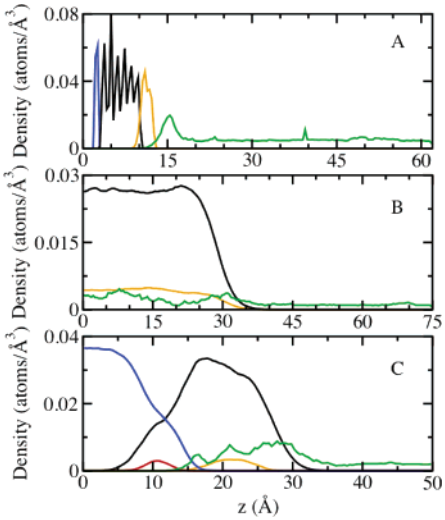

Figure 6. Density profiles in the direction normal to the interface between the vapor and the organic media for the (A) SAM, (B) C14ENE, and (C) OPPC systems with ozone. The ozone center of mass (green) density profile in each panel is multiplied by 100 for scaling. The other colors correspond to the same atoms as in Figure 2. Note the different scales in each panel.

SASA analysis, a spherical probe is used to determine the percentage of the total accessible surface area that is occupied by double bonds. A probe radius of 2.0 Å is selected as a reasonable representation of the size of an ozone molecule. This analysis is performed for system configurations every 1.0 ps, and the average percentage is calculated. This percentage is a measure of the likelihood that an incoming gas phase ozone molecule will encounter a double bond on the surface.

The percentage of the total accessible surface area that is due to double bonds has been reported previously for the OPPC system as 3.7%.[2] The small amount of double bond surface exposure is due to the internal double bond of the OPPC molecule. The percentages from the SAM and C14ENE systems are 99.7 and 28.5%, respectively. The essentially complete coverage by double bonds in the SAM system is expected on the basis of the terminal double bond of 1-octenethiolate and the density profile in panel A of Figure 2. The double bond surface exposure to an ozone molecule in the C14ENE system is almost 2 times larger than expected on the basis of the percentage of total carbons that are part of a double bond in a 1-tetradecene molecule, which is 14%. This is due in part to the molecular orientation of the 1-tetradecene molecules located at the interface (panel B of Figure 3), which prefer to lie flat on the surface.

B. Ozone Uptake and Collision Dynamics. Following the addition of the ozone molecules to the neat systems and equilibration, the positions of the ozone molecules are monitored. The density profiles that are generated from these simulations are shown in Figure 6 for the SAM (top panel), C14ENE (middle panel), and OPPC (bottom panel) systems. The ozone molecules penetrate only a few angstroms into the SAM and reside predominantly on the surface of the film. The ozone molecules in the C14ENE system are located in both the bulk liquid and at the liquid/vapor interface. In the OPPC system, the ozone molecules are located primarily in the lipid portion of the monolayer but do not penetrate into the water. This is consistent with the lower solubility of ozone in water than in organic liquids.[55,56] From the data in Figure 6, the minimum z positions reached by an ozone molecule are 9.8, 0, and 12 Å in the SAM, C14ENE, and OPPC systems, respectively. It is clear from the data in Figure 6 that the major factor

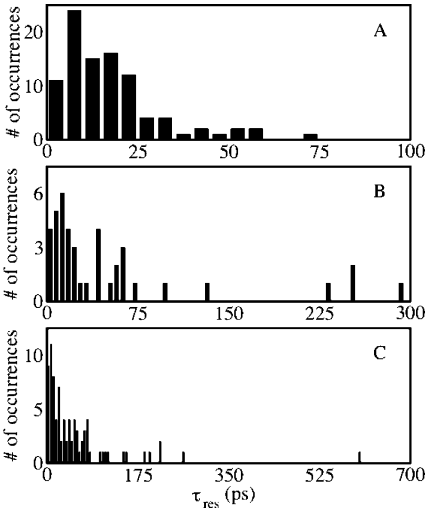

Figure 7. Probability distributions of ozone residence times in the (A) SAM, (B) C14ENE, and (C) OPPC systems. The tick marks are removed for clarity. Note the different scales in each panel.

TABLE 1: Average Residence Time of Ozone in the Organic Phase and the Percent Contribution from the Bulk and Interface

system	$\langle\tau_{res}\rangle$ (ps)	bulk (%)	interface (%)
SAM	17		
C14ENE	53	39	61
OPPC	55	37	63

determining whether ozone diffuses into the interior of the organic phase is the density at the interface.

The amount of time that an ozone molecule interacts with the organic media before returning to the gas phase is defined as the residence time, τ_{res}. Specifically, τ_{res} is determined by the continuous amount of time that the z value of an ozone molecule's center of mass is less than the observed minimum z value for desorption to occur, which are determined to be 20, 40, and 36 Å in the SAM, C14ENE, and OPPC systems, respectively. These z values are used to define the residence time because ozone molecules with a z value greater than this desorbed into the vapor. The probability distributions of the residence times are shown in Figure 7 for the three systems. The average residence times are calculated from the distributions in Figure 7 and reported in Table 1. In the C14ENE and OPPC systems, the percentages of τ_{res} that are due to the time spent in the bulk and interface are shown in Table 1 also. The z values used to separate the bulk from the interface are 25 and 24 Å in the C14ENE and OPPC systems, respectively, which correspond to 90% of the maximum total carbon density.

The maximum residence time in the SAM system is less than 75 ps, but ozone molecules can reside in the organic media of the C14ENE and OPPC systems for several hundreds of picoseconds. The average residence times in the C14ENE and OPPC systems are a factor of 3 larger than in the SAM system because of the uptake of ozone into the interior of the organic media. This is supported by the minimum z values given above and by plots of the center of mass of each ozone molecule as a function of time (data not shown). The average residence times and percentage of the residence time spent in bulk and interface are nearly identical for the C14ENE and OPPC systems. This indicates that the environment an ozone molecule interacts with is similar in the C14ENE and OPPC systems, which is supported by the structural similarities discussed in section III.A.

TABLE 2: Ozone−Double Bond Collision Rates with $R_c = 4$ Å and the Percent Contribution from the Bulk and Interface

system	C_{db} (s^{-1} cm^{-2} ppm^{-1}) × 10^{17}	bulk (%)	interface (%)
SAM	20		100
C14ENE	39	85	15
OPPC	3.8	61	39
theory	2.2		100

During the residence time of the ozone molecules, the total number of collisions between ozone molecules and double bonds is counted, and the collision rate, C_{db}, is determined by dividing the total number of collisions by the total trajectory time. A collision event is defined as the ozone center of mass being less than a specified cutoff distance, R_c, from the center of a double bond. If the ozone molecule remains less than R_c from a double bond for a continuous period of time, only a single collision event is counted, and the collision lifetime is measured. (See below.) The sensitivity of C_{db} to the value of R_c was tested using $R_c = 4$, 5, and 6 Å. The results with a value of 4 Å are selected for several reasons. Each ozone molecule is undergoing on average a single collision event with only the nearest alkene when $R_c = 4$ Å, whereas larger values of R_c increase C_{db} because the ozone molecules are involved in multiple collision events simultaneously. Another reason for using $R_c = 4$ Å is that ab initio calculations of ozone and ethylene show that there is a stable complex on the reaction path formed at a center of mass separation of 3.291 Å.[26]

The values of C_{db} with $R_c = 4$ Å and the percentages of the collisions that occur in the bulk and interface are reported in Table 2. C_{db} is normalized by the total surface area and the gas phase ozone concentration in each system. The same threshold z values described above for τ_{res} are used to define the bulk and interface regions. The data in Table 2 show that the largest number of ozone−double bond collisions occurs in the C14ENE system and that these collisions are primarily in the bulk liquid. The large number of ozone−double bond collisions results from the double bonds being dispersed throughout the organic medium and the uptake of the ozone molecules into the bulk liquid. The data in Figures 6 and 7 and Table 1 indicate that the uptake into the organic phase and residence time of ozone molecules in the OPPC system are similar to those for the C14ENE system. Therefore, the reduction of C_{db} by a factor of 10 in the OPPC system relative to the value for the C14ENE system is attributed to the localization of the double bonds in the interior of the organic medium. In the SAM system, the double bonds are localized at the organic surface, and the ozone molecules reside at the surface without uptake into the interior of the monolayer. This results in a reduction of C_{db} by a factor of 2 relative to the value for the C14ENE system. The observed collision rates result from the interplay of several factors: the location of the double bonds, the uptake of ozone into the organic phase, and the residence time of ozone.

The collision rates from the simulations are compared in Table 2 to the collision rate predicted by gas−surface collision theory:

$$C = A[O_3]\sqrt{\frac{RT}{2\pi M}} \qquad (2)$$

In eq 2, A is the surface area, $[O_3]$ is the gas phase ozone concentration, R is the gas constant, T is the temperature, and M is the molecular mass of ozone. All three systems exhibit an enhancement in the collision rate relative to the prediction from theory. However, the theoretical collision rate should be an upper

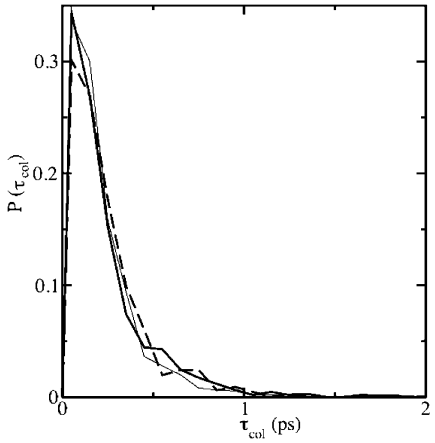

Figure 8. Probability distributions of collision lifetimes in the SAM (thick solid), C14ENE (thin solid), and OPPC (dashed) systems.

bound because gas−surface collision theory assumes that every surface collision of a gas phase ozone molecule is with a double bond. This is a reasonable assumption for the SAM system; however, the theory does not account for the residence time of ozone on the SAM surface, which results in an enhancement by a factor of 9 relative to theory. In the C14ENE and OPPC systems, the enhancement relative to theory is due to the trapping of ozone molecules in the organic phase, where they undergo multiple collisions with double bonds. The average number of collisions between an ozone molecule and double bonds per collision with the surface in the SAM, C14ENE, and OPPC systems is 12, 67, and 8, respectively.

Although the ozone−double bond collision rate differs between the three systems, the ozone−double bond collision lifetime is independent of the system being considered. The collision lifetime, τ_{col}, is defined as the amount of time that an ozone molecule's center of mass is less than $R_c = 4$ Å away from the center of a double bond. The probability distributions of collision lifetimes, $P(\tau_{col})$, are shown in Figure 8 for the three systems. The average collision lifetime is 0.2 ps in all three systems. Although the collision rate is sensitive to the structure of the organic phase, the lifetime of the collision is dominated by the short-range interaction between an ozone molecule and a double bond.

C. Comparison with Experimental Results. Moise and Rudich recently published uptake measurements of ozone with organic liquids and SAMs containing terminal alkenes.[18] Despite the larger double bond density at the SAM surface relative to that at a liquid surface, the uptake probability of ozone is 1 order of magnitude larger in the liquid than in the SAM. The enhancement in the liquid is attributed to additional processes occurring in the bulk, such as solubility, diffusion, and reaction, which do not occur in the SAM system.

The simulation results are consistent with the conclusions from that experiment. In the simulations, the ozone molecules are absorbed into the liquid and reside there 3 times longer than on the surface of the SAM (53 ps compared to 17 ps). In addition to solubility, the simulations suggest that ozone molecules are removed more efficiently from the liquid system than from the SAM system because of a faster rate of collision with double bonds. The data in Table 2 show that ozone molecules in the C14ENE system are colliding almost 2 times faster with double bonds than in the SAM system. An even larger rate enhancement in the liquid is predicted if a shorter alkene than 1-tetradecene is used, thus increasing the ratio of alkene carbon to alkane carbon. Both uptake in the liquid phase and a larger ozone−double bond collision rate in the liquid are consistent with a larger uptake probability in organic liquids relative to that in SAMs.

TABLE 3: Comparison of Simulation and Experimental Results for the Reaction of Ozone with the OPPC System

	C_{db} (s^{-1}) $\times 10^{20}$	reaction completion time (min)
experiment	1.7	5.5
simulation	2.9	2.8

The experimental kinetics of gas phase ozone reacting with a phospholipid monolayer of OPPC molecules have been reported recently.[2] A reaction probability that is 1 order of magnitude larger than expected on the basis of an analogous gas phase reaction is obtained. The enhancement in the reaction probability is attributed to the trapping of the ozone molecules in the organic film, which is supported by the simulation results. The experimental finding is supported by a recent publication on the heterogeneous reaction of ozone at the liquid/vapor interface of oleic, linoleic, and linolenic acid.[4] An enhancement of the reaction probability by 3 orders of magnitude is estimated at the surface of oleic acid relative to analogous gas phase reactions. Moise and Rudich also reported an enhancement in the reaction probability for ozone with an alkene-terminated self-assembled monolayer by 3 orders of magnitude relative to that in the gas phase.[57]

A quantitative comparison between the experimental and simulation results can be made for the OPPC system. In the experiment, eq 1 is solved for the reaction probability, Γ, using the experimental reaction rate, R, and a collision rate, C, from eq 2 with the experimental conditions of $A = 772$ cm^2, $[O_3] =$ 1 ppm, and $T = 300$ K. The collision rate used in the experimental calculations is compared to the collision rate from simulations (after scaling to correspond with A and $[O_3]$ employed in the experiment) in Table 3. The collision rate from simulations is enhanced by a factor of 1.7 relative to gas−surface collision theory. This results in a shorter predicted time for the completion of the reaction than observed in the experiment, which is shown in Table 3 also.

The agreement between the experimental and simulation results for the OPPC system is reasonable and supports the conclusion of enhanced reaction kinetics at the interface relative to the gas phase. If a gas phase reaction probability applied to this system, then the time for reaction completion would be approximately a factor of 10 larger than the values in Table 3. The agreement between experimental and simulation results is important for several other reasons. It indicates that the simulation model of the OPPC system with ozone provides a realistic description of the experimental system. Also, it supports using a 4-Å separation as the criterion for an ozone−double bond collision event. In future work, a quantitative comparison between experimental and simulation results of ozone reacting with different length alkene-terminated SAMs will be made.[58]

IV. Conclusions and Atmospheric Implications

The molecular dynamics simulations results presented here are relevant to environmental and biological systems containing unsaturated organic compounds at interfaces with air that are subject to processing by gas phase oxidants. The structure of three different organic systems is characterized and correlated with the uptake and collision dynamics of gas phase ozone molecules. The density profile, molecular orientation, and double bond orientation for the three different organic systems indicate

that the SAM has characteristics similar to those of a solid surface, whereas the OPPC monolayer is similar in structure to the C14ENE liquid system.

The organic density at the surface controls the uptake of ozone into the organic phase, which occurs in the C14ENE and OPPC systems. Although uptake into the organic phase does not occur in the SAM system, the van der Waals interaction between ozone and the SAM results in a significant residence time in the surface region. The residence times in the C14ENE and OPPC systems are 3 times larger than in the SAM system because of uptake into the interior of the organic phase.

The collision rate between an ozone molecule and a double bond is sensitive to the structure of the organic system. The trend in collision rates from largest to smallest is C14ENE > SAM > OPPC. The collision rate is largest when the double bonds are dispersed throughout the organic phase and the uptake of ozone into the organic phase occurs. Localization of the double bonds in the monolayer systems results in smaller collision rates than in the liquid. The collision rates in the monolayer systems are dependent also on the location of the localized double bonds relative to the distance ozone diffuses into the organic phase.

The collision rates from the three systems are larger than the prediction from gas−surface collision theory by factors ranging from 1.7 to 18. The average collision lifetime is 0.2 ps in all three systems and is not sensitive to the organic structure. The overall agreement with several experiments supports the models and the definition of a collision event used in the simulations. Also, the simulation results support the experimental finding of enhanced kinetics for the reaction of ozone with double bonds at OPPC monolayers relative to that for the gas phase.

The results of these simulations are relevant to the oxidative processing of tropospheric organic aerosols because each system represents a model for a particular type of organic aerosol. The SAM system represents an organic layer adsorbed on an inorganic core, such as a mineral dust particle,[59] the OPPC system represents an organic layer adsorbed on an aqueous core,[60] and the C14ENE system represents an aerosol composed of an organic liquid.[61,62] It is likely that the simulated systems are an idealized representation of analogous experimental systems and of atmospheric organic aerosols. However, an important result is that the collision rates in Table 2 for the three different systems span 1 order of magnitude. This indicates that the rate of oxidative processing of organic aerosols is sensitive to the detailed molecular structure of the aerosol particle. The simulations predict that dramatic differences in the rate of ozone depletion, volatile product formation, and modification of organic aerosol physical properties may exist depending on the organic aerosol structure. Further simulations of these systems may focus on incorporating a degree of disorder into the organic systems that more accurately describes naturally occurring organic aerosols. In the SAM system, this can be accomplished by randomly removing some of the hydrocarbon molecules from the system, thus creating vacancies on the gold surface. This may have interesting effects on the SAM structure and on the trapping of gas phase molecules in the interior of the monolayer.

Acknowledgment. A Collaborative Research in Chemistry grant from the National Science Foundation (CHE-0209719) has supported this work. We thank Professor Barbara J. Finlayson-Pitts, Professor R. Benny Gerber, Professor John C. Hemminger, Dr. Yael Dubowski, Dr. Martina Roeselova, and Dr. Chris Knox for helpful discussions. O.L.M. thanks the Undergraduate Research Opportunities Program at UC Irvine for a Summer Undergraduate Research Fellowship.

References and Notes

(1) Knipping, E. M.; Lakin, M. J.; Foster, K. L.; Jungwirth, P.; Tobias, D. J.; Gerber, R. B.; Dabdub, D.; Finlayson-Pitts, B. J. *Science* **2000**, *288*, 301.

(2) Wadia, Y.; Tobias, D. J.; Stafford, R.; Finlayson-Pitts, B. J. *Langmuir* **2000**, *16*, 9321.

(3) Laskin, A.; Gaspar, D. J.; Wang, W.; Hunt, S. W.; Cowin, J. P.; Colson, S. D.; Finlayson-Pitts, B. J. *Science* **2003**, *301*, 340.

(4) Thornberry, T.; Abbatt, J. P. D. *Phys. Chem. Chem. Phys.* **2004**, *6*, 84.

(5) Novakov, T.; Penner, J. E. *Nature* **1993**, *365*, 823.

(6) Murphy, D. M.; Thomson, D. S.; Mahoney, M. J. *Science* **1998**, *282*, 1664.

(7) Tervahattu, H.; Juhanoja, J.; Kupiainen, K. *J. Geophys. Res.* **2002**, *107*, 4319.

(8) Saxena, P.; Hildemann, L. M.; McMurry, P. H.; Seinfeld, J. H. *J. Geophys. Res.* **1995**, *100*, 18755.

(9) Marty, J. C.; Saliot, A.; Buat-Menard, P.; Chesselet, R.; Hunter, K. A. *J. Geophys. Res.* **1979**, *84*, 5707.

(10) Notter, R. H. *Lung Surfactants: Basic Science and Clinical Applications*; Marcel Dekker: New York, 2000.

(11) Podgorski, A.; Sosnowski, T. R.; Gradon, L. *J. Aerosol Med.* **2001**, *14*, 455.

(12) Wildt, J.; Kobel, K.; Schuh-Thomas, G.; Heiden, A. C. *J. Atmos. Chem.* **2003**, *45*, 173.

(13) Purves, W. K.; Orians, G. H.; Heller, H. C. *Life: The Science of Biology*, 3rd ed.; Sinauer Associates, Inc.: Sunderland, MA, 1992.

(14) de Gouw, J. A.; Lovejoy, E. R. *Geophys. Res. Lett.* **1998**, *25*, 931.

(15) Tobias, H. J.; Ziemann, P. J. *Environ. Sci. Technol.* **2000**, *34*, 2105.

(16) Tobias, H. J.; Docherty, K. S.; Beving, D. E.; Ziemann, P. J. *Environ. Sci. Technol.* **2000**, *34*, 2116.

(17) Orlando, J. J.; Noziere, B.; Tyndall, G. S.; Orzechowska, G. E.; Paulson, S. E.; Rudich, Y. *J. Geophys. Res.* **2000**, *105*, 11.

(18) Moise, T.; Rudich, Y. *J. Geophys. Res.* **2000**, *105*, 14667.

(19) Thomas, E. R.; Frost, G. J.; Rudich, Y. *J. Geophys. Res.* **2001**, *106*, 3045.

(20) Moise, T.; Rudich, Y. *J. Phys. Chem A* **2002**, *106*, 6469.

(21) Morris, J. W.; Davidovits, P.; Jayne, J. T.; Jimenez, J. L.; Shi, Q.; Kolb, C. E.; Worsnop, D. R.; Barney, W. S.; Cass, G. *Geophys. Res. Lett.* **2002**, *29*, 1357.

(22) Eliason, T. L.; Aloisio, S.; Donaldson, D. J.; Cziczo, D. J.; Vaida, V. *Atmos. Environ.* **2003**, *37*, 2207.

(23) Mmereki, B. T.; Donaldson, D. J. *J. Phys. Chem A* **2003**, *107*, 11038.

(24) Rudich, Y. *Chem. Rev.* **2003**, *103*, 5097.

(25) Finlayson-Pitts, B. J.; Pitts, J. N. *Chemistry of the Upper and Lower Atmosphere: Theory, Experiments, and Applications*; Academic Press: San Diego, CA, 2000.

(26) Gillies, C. W.; Gillies, J. Z.; Suenram, R. D.; Lovas, F. J.; Kraka, E.; Cremer, D. *J. Am. Chem. Soc.* **1991**, *113*, 2412.

(27) Ljubic, I.; Sabljic, A. *J. Phys. Chem A* **2002**, *106*, 4745.

(28) Wilson, M. A.; Pohorille, A. *J. Phys. Chem B* **1997**, *101*, 3130.

(29) Taylor, R. S.; Garrett, B. C. *J. Phys. Chem B* **1999**, *103*, 844.

(30) Roeselova, M.; Jungwirth, P.; Tobias, D. J.; Gerber, R. B. *J. Phys. Chem B* **2003**, *107*, 12.

(31) Lipkin, N.; Gerber, R. B.; Moiseyev, N.; Nathanson, G. M. *J. Chem. Phys.* **1994**, *100*, 8408.

(32) Benjamin, I.; Wilson, M.; Pohorille, A. *J. Chem. Phys.* **1994**, *100*, 6500.

(33) Benjamin, I.; Wilson, M. A.; Pohorille, A.; Nathanson, G. M. *Chem. Phys. Lett.* **1995**, *243*, 222.

(34) Morita, A. *Chem. Phys. Lett.* **2003**, *375*, 1.

(35) Chorny, I.; Benjamin, I.; Nathanson, G. M. *J. Phys. Chem. B* **2004**, *108*, 995.

(36) Tobias, D. J.; Tu, K.; Klein, M. L. *J. Chim. Phys.* **1997**, *94*, 1482.

(37) Mar, W.; Klein, M. L. *Langmuir* **1994**, *10*, 188.

(38) Brooks, B. R.; Bruccoleri, R. E.; Olafson, B. D.; States, D. J.; Swaminathan, S.; Karplus, M. *J. Comput. Chem.* **1983**, *4*, 187.

(39) Feller, S. E.; MacKerell, A. D. *J. Phys. Chem. B* **2000**, *104*, 7510.

(40) Tuckerman, M. E.; Yarne, D. A.; Samuelson, S. O.; Hughes, A. L.; Martyna, G. J. *Comput. Phys. Commun.* **2000**, *128*, 333.

(41) Lide, D. R. *CRC Handbook of Chemistry and Physics*, 73rd ed.; CRC Press: Boca Raton, FL, 1992.

(42) Jasper, J. J.; Kerr, E. R. *J. Am. Chem. Soc.* **1954**, *76*, 2659.

(43) MacKerell, A. D.; Bashford, D.; Bellott, M.; Dunbrack, R. L.; Evanseck, J. D.; Field, M. J.; Fischer, S.; Gao, J.; Guo, H.; Ha, S.; Joseph-McCarthy, D. J.; Kuchnir, L.; Kuczera, K.; Lau, F. T. K.; Mattos, C.; Michnick, S.; Ngo, T.; Nguyen, D. T.; Prodhom, B.; Reiher, W. E.; Roux,

B.; Schlenkrich, M.; Smith, J. C.; Stote, R.; Straub, J.; Watanabe, M.; Wiorkiewicz-Kuczera, J.; Yin, D.; Karplus, M. *J. Phys. Chem. B* **1998**, *102*, 3586.

(44) Meerts, W. L.; Stolte, S.; Dymanus, A. *Chem. Phys.* **1977**, *19*, 467.

(45) Mack, K. M.; Muenter, J. S. *J. Chem. Phys.* **1977**, *66*, 5278.

(46) Trambarulo, R.; Gosh, S. N.; Burrus, C. A.; Gordy, W. *J. Chem. Phys.* **1953**, *21*, 851.

(47) Leach, A. R. *Molecular Modelling: Principles and Applications*; Addison-Wesley Longman Limited: Essex, U.K., 1996.

(48) Martyna, G. J.; Tuckerman, M. E.; Tobias, D. J.; Klein, M. L. *Mol. Phys.* **1996**, *87*, 1117.

(49) Essmann, U.; Perera, L.; Berkowitz, M. L.; Darden, T.; Lee, H.; Pedersen, L. G. *J. Chem. Phys.* **1995**, *103*, 8577.

(50) Ryckaert, J. P.; Ciccotti, G.; Berendsen, H. C. *J. Comput. Chem.* **1977**, *23*, 327.

(51) Andersen, H. C. *J. Comput. Chem.* **1983**, *52*, 24.

(52) Humphrey, W.; Dalke, A.; Schulten, K. *J. Mol. Graphics* **1996**, *14*, 33.

(53) Ulman, A. *Chem. Rev.* **1996**, *96*, 1533.

(54) Lee, B.; Richards, F. M. *Mol. Biol.* **1971**, *55*, 379.

(55) Kosak-Channing, L. F.; Heiz, G. R. *Environ. Sci. Technol.* **1983**, *17*, 145.

(56) Razumovskii, S. D.; Zaikov, G. E. *Ozone and Its Reactions with Organic Compounds*; Elsevier: Amsterdam, 1984.

(57) Moise, T.; Rudich, Y. *Geophys. Res. Lett.* **2001**, *28*, 4083.

(58) Dubowski, Y.; Vieceli, J.; Tobias, D. J.; Finlayson-Pitts, B. J. To be submitted for publication.

(59) Usher, C. R.; Michel, A. E.; Grassian, V. H. *Chem. Rev.* **2003**, *103*, 4883.

(60) Ellison, G. B.; Tuck, A. F.; Vaida, V. *J. Geophys. Res.* **1999**, *104*, 11.

(61) Jang, M.; Kamens, R. M.; Leach, K. B.; Strommen, M. R. *Environ. Sci. Technol.* **1997**, *31*, 2805.

(62) Liang, C.; Pankow, J. F.; Odum, J. R.; Seinfeld, J. H. *Environ. Sci. Technol.* **1997**, *31*, 3086.